2008 IEEE Region 10 Colloquium and the Third International Conference on Industrial and Information Systems, Kharagpur, INDIA December 8 -10, 2008.
330

Performance Evaluation of a Sensorless Induction Motor Drive at Very Low and Zero Speed Using a MRAS Speed Observer

Shady M. Gadoue, *Member, IEEE,* Damian Giaouris, *Member, IEEE,* and John W. Finch, *Senior Member, IEEE*
School of Electric Electronic and Computer Engineering
Newcastle University
Newcastle upon Tyne, UK
e-mail: shady.gadoue@ncl.ac.uk, damian.giaouris@ncl.ac.uk, j.w.finch@ncl.ac.uk

***Abstract*— Model Reference Adaptive System (MRAS) represents one of the most attractive and popular solutions for sensorless control of AC drives. However, the performance of this scheme deteriorates when approaching the zero speed zone. This paper presents an experimental evaluation of the performance of MRAS speed observer when working at very low and zero speed. Results are obtained when applied to an indirect vector control induction motor drive in both open loop and sensorless modes of operation. Since the focus here is on operation around and at zero speed under both no-load and loading operating conditions, this represents a useful contribution to the literature. Results show the deterioration in the performance of the estimation scheme at very low and zero speed especially when load is applied.**

Keywords- Induction motor; MRAS; sensorless control

I. INTRODUCTION

Several solutions for sensorless control of AC drives have been proposed based on the machine fundamental excitation model, as summarized recently [1]. These algorithms use the instantaneous values of stator voltages and currents to estimate the flux linkage and the motor speed. Various techniques have been suggested such as: Model Reference Adaptive Systems (MRAS), Luenberger and Kalman-filter observers, sliding-mode observers and Artificial Intelligence (AI) techniques. MRAS schemes offer simpler implementation and require less computational effort compared to other methods and are therefore the most popular strategies used for sensorless control [2].

Various MRAS observers have been introduced in the literature based on rotor flux, back EMF and reactive power [3-5]. However, rotor flux MRAS, first proposed by Schauder [4], is the most popular MRAS strategy and a lot of effort has been focused on improving the performance of this scheme. This scheme suffers from stator resistance sensitivity and pure integration problems which may cause dc drift and initial condition problems [5]. These problems may limit the performance at low and zero speed region of operation [3]. In [6], a simultaneous estimation of rotor speed and stator resistance is presented based on a parallel MRAS observer where both the reference and adaptive models switch roles based on two adaptive mechanisms. an Artificial NN (ANN) is used with MRAS in [7] to detect the thermal variations in the stator resistance at different operating conditions. Low-Pass Filters (LPF) with low cut-off frequency have been proposed to replace the pure integrator [8]. This introduces phase and gain errors and delays the estimated speed relative to the actual, which may affect the dynamic performance of the drive in addition to inaccurate speed estimation below the cut-off frequency [5, 9]. To overcome this problem, Karanayil et al [9] introduces a programmable cascaded low pass filter (PCLPF) to replace the pure integration by small time constant cascaded filters to attenuate the dc offset decay time. In [10], another technique is used where the rotor flux is estimated by defining a modified integrator having the same frequency response as the pure integrator at steady state. The Neural Network (NN) has been presented as an adaptive filter used for signal integration to eliminate the offset in the flux integration for the voltage model flux observer [11]. A nonlinear feedback integrator for drift and dc offset compensation has been proposed in [12]. Further research has tried to entirely replace the voltage model with a full order stator and rotor flux observer which reduces the scheme's simplicity [13] .

Moreover, Neural Networks (NN) have been proposed to replace the conventional adaptive model used in rotor flux-MRAS [8]. A two layer linear neural network is proposed to represent the conventional adaptive current model (CM) using a simple forward Euler integration method [8]. The estimated speed represents one of the neural network weights updated online using a back propagation algorithm. An evolution to this scheme is presented in [14, 15] where an Adaptive linear NN (ADALINE) is employed in the adaptive model using modified Euler integration to represent the CM. The Ordinary Least Square (OLS) algorithm is used to train the NN online to obtain the rotor speed information. Another approach is discussed in [16] using a sliding mode flux observers in the adaptive model

IEEE Kharagpur Section & IEEE Sri Lanka Section

and deduces a speed estimation law based on sliding mode theory.

Despite the considerable research in the area of sensorless control it is still a lack of results devoted to the performance of MRAS scheme at very low and zero speed. The need for systematic testing in this region has been highlighted recently [1]. This paper presents a detailed experimental evaluation of the performance of such a scheme at very low and zero speed with and without load, and is hence a useful contribution to rectifying this deficiency.

II. ROTOR FLUX MRAS SPEED OBSERVER

The classical rotor flux MRAS speed observer structure shown in Fig. 1 consists of a reference model, an adaptive model, and an adaptation scheme which generates the estimated speed. The reference model, usually expressed as a VM, represents the stator equation. It generates the reference value of the rotor flux components in the stationary reference frame from the stator voltage (estimated to avoid a direct measurement as discussed later) and monitored current components. The reference rotor flux components obtained from the reference model are given by [4, 5]:

$$p\psi_{rd} = \frac{L_r}{L_m}(v_{sd} - R_s i_{sd} - \sigma L_s p i_{sd}) \quad (1)$$

$$p\psi_{rq} = \frac{L_r}{L_m}(v_{sq} - R_s i_{sq} - \sigma L_s p i_{sq}) \quad (2)$$

where σ is the leakage coefficient given by:

$$\sigma = 1 - \frac{L_m^2}{L_s L_r} \quad (3)$$

The adaptive model, usually represented by the CM, describes the rotor equation where the rotor flux components are expressed in terms of stator current components and the rotor speed. The rotor flux components obtained from the adaptive model are given by [4, 5]:

$$p\hat{\psi}_{rd} = \frac{L_m}{T_r} i_{sd} - \frac{1}{T_r}\hat{\psi}_{rd} - \hat{\omega}_r \hat{\psi}_{rq} \quad (4)$$

$$p\hat{\psi}_{rq} = \frac{L_m}{T_r} i_{sq} - \frac{1}{T_r}\hat{\psi}_{rq} + \hat{\omega}_r \hat{\psi}_{rd} \quad (5)$$

Based on Popov's hyperstability criterion, the adaptation mechanism can be designed to generate the value of the estimated speed used so as to minimize the error between the reference and estimated fluxes [5]. In the classical RF-MRAS scheme, this is done by defining a speed tuning signal, ε_ω, minimized by a PI controller which generates the estimated speed which is fed back to the adaptive model. The expressions for the speed tuning signal and the estimated speed can be given as [5]:

$$\varepsilon_\omega = \psi_{rq}\hat{\psi}_{rd} - \psi_{rd}\hat{\psi}_{rq} \quad (6)$$

$$\hat{\omega}_r = (k_p + \frac{k_i}{p})\varepsilon_\omega \quad (7)$$

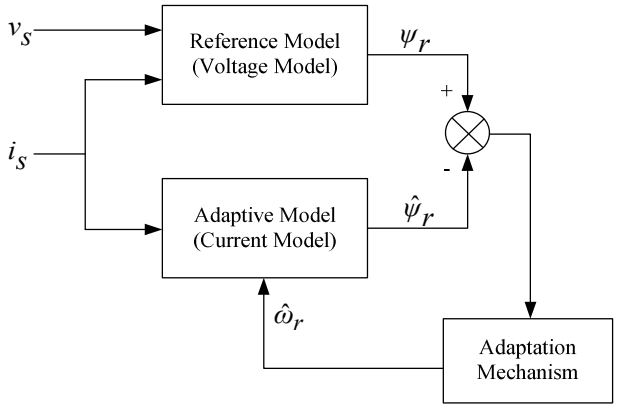

Fig. 1 Rotor flux-MRAS speed observer

III. PROBLEMS AT LOW SPEED

A. Parameter sensitivity

Since the speed estimation is based on the machine model, it is highly sensitive to machine parameter variations. Stator resistance variation with machine temperature is a most serious problem at low speed. Since the fundamental component of the stator voltage becomes very low, the stator resistance drop becomes comparable to the applied voltage. Hence continuous adaptation of the stator resistance is required to maintain stable operation at low speed.

B. Stator voltage acquisition and inverter nonlinearity

Stator voltage measurement comes up due to sensorless control. The stator voltage signal is crucial for model based strategies. The most accurate stator voltage acquisition is that measured across the machine terminals. This cannot be used easily since it requires a very high sampling rate [17]. Low pass filtering the PWM voltage waveform may solve the problem at medium and high speed but not at low speed, where the effect of filter gain and phase error causes performance to deteriorate. Another nonlinear filtering technique known as synchronous integrator technique can aid a solution [18]. This technique is based on integrating the PWM voltage signal and resetting at the end of the PWM period. This provides the actual volts-seconds applied on machine terminal over PWM period. This technique should provide better measurement including all inverter nonlinearities [18]. However, not using voltage sensors is preferred in industrial applications. Using the reference voltages, available in the control unit, is possible since they are harmonic free. However, at low speed these reference voltages deviate substantially from the actual machine voltages due to inverter dead time effects and inverter nonlinearities due to the characteristics of the power switches including threshold voltages and voltage drops. Holtz and Quan [19] has modeled the inverter nonlinearities including voltage drops across the switches and the threshold voltage and hence a better acquisition of the stator voltage is obtained from the reference voltage of the PWM inverter at very low speed.

C. *Stator current acquisition and pure integration problems*

Errors in the measured currents can be due to unbalanced gains of the measurement channels, DC offset and drift. This may cause oscillation in the measured speed [19, 20].

Rotor flux estimation based on VM needs open loop integration for flux calculation. This pure integration is difficult to implement because of DC drift and initial condition problems. Replacement of pure integration by a low pass filter may help [5, 10, 11]. However, the flux estimation deteriorates below the filter cut-off frequency [5].

IV. EXPERIMENTAL SETUP

The experimental platform, shown in Fig. 2, consists of a 7.5 kW, 415 V, delta connected three phase induction machine loaded by a 9 kW, 240 V, 37.5 A separately excited DC load machine to allow separate control of torque and speed of the DC machine. A 15 kW four quadrant DC drive from the Control Techniques "Mentor" range is used to control the DC machine to provide different levels of loading on the induction machine up to full load. The induction machine parameters are given in Table I.

The AC drive power electronics consists of a 50A 3 Phase Diode Bridge and 1200V, 50A half bridge IGBT power modules. To control the induction motor a dSPACE system is used which contains a PowerPC 604e running at 400 MHz, and a Slave TMS320F240 DSP. The actual motor speed is measured by a 5000 pulses/revolution speed encoder. The inverter switching frequency is 15 kHz and the vector control is executed with the same sampling frequency. The observer and the speed control loop have a sampling frequency of 5 kHz and the speed measurement is executed with a sampling frequency of 250 Hz.

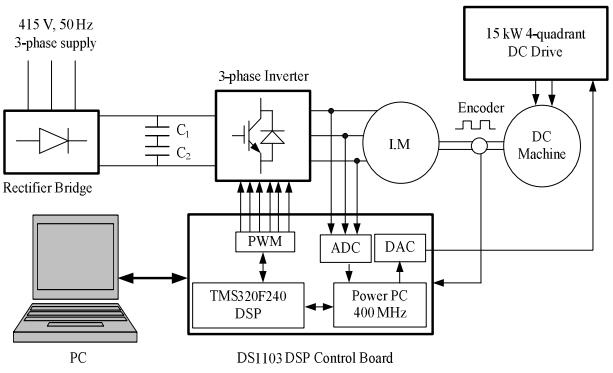

Fig. 2 Experimental setup

During practical implementation of the MRAS scheme it was found necessary to cascade a low cut-off frequency HPF at the outputs of the voltage model to remove integrator drift and any initial condition problems. The cut-off frequency should be selected as low as possible since the purpose is just to remove the DC component and therefore a value of 1 Hz is chosen. A simple dead time compensator similar to [21, 22] is implemented and reference voltages which are available in the control unit are used as the real stator voltages and will be used for voltage model flux observer in (1) and (2).

V. EXPERIMENTAL RESULTS

Extensive experimental tests were carried out to evaluate the performance of MRAS observer using an indirect vector control induction motor drive. The tests were performed in both open loop and sensorless modes of operation. Selected experimental results from these tests are shown in the following sections.

A. *Open loop performance*

The speed estimation scheme was tested in open loop when the drive is operated as encodered vector control, i.e. the encoder speed is used for speed control and rotor flux angle estimation. The drive was subjected to different reference speed changes at various load torque levels. The PI controller gains can be selected as high as possible but are limited by the noise [5]. Values of $k_p = 10$ and $k_i = 100$ are selected. Figs. 3-4 show the open loop performance of MRAS scheme and model outputs for ±50 rpm speed reversal at no-load and for 12.5% load torque disturbance rejection at 30 rpm.

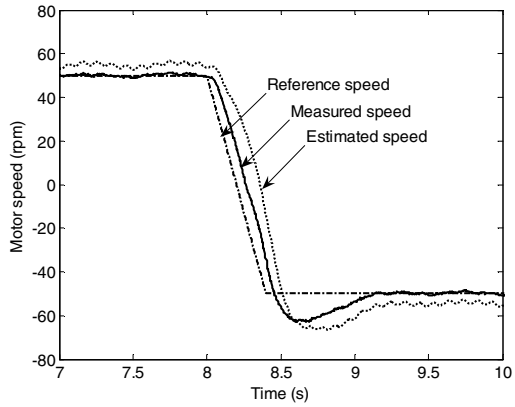

(a)

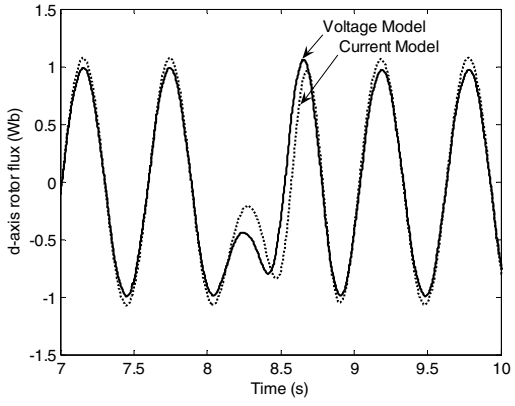

(b)

Fig. 3 Open loop ±50 rpm speed reversal, no-load. (a) Estimated speed (b) MRAS outputs

At low speed a steady state error in the estimated speed is observed for the conventional MRAS observer. This is mainly due to the stator resistance mismatch between the motor and the observer. Moreover, dead time effects cannot be completely removed even by complicated compensation schemes [17]. So the reference voltages used for the voltage model do not match the actual stator voltages across the machine terminals representing another source for the steady state error in the estimated speed.

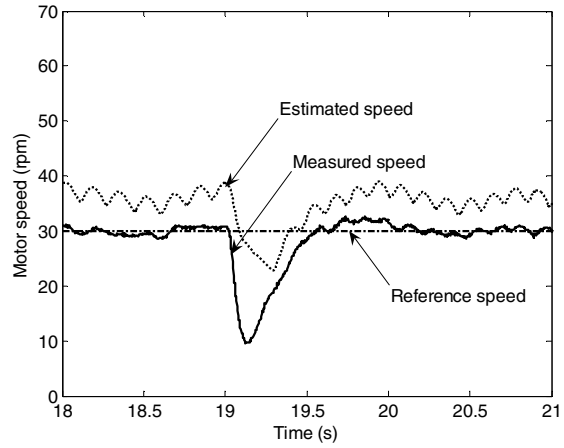

(a)

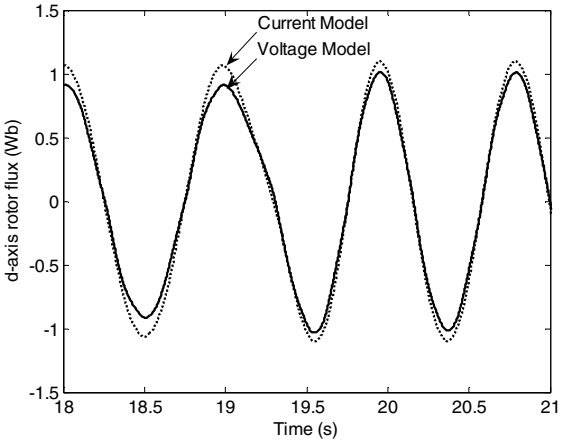

(b)

Fig. 4 Open loop 12.5% load torque disturbance rejection, 30 rpm. (a) Estimated speed (b) MRAS outputs

B. *Sensorless performance*

In the following tests, the estimated speed is used for speed control and field orientation where the drive is working as sensorless indirect rotor flux oriented. The encoder speed is used for comparison purpose only. Tests are conducted in the low speed and at or around the zero speed region based on some benchmark tests described in [12, 23, 24]. The same PI gains will be used. Selected experimental results for the tests are shown in the following section.

Fig. 5 shows the result of a test where the sensorless vector control drive is subjected to stair case speed demand from 100 rpm to zero speed in a series of five 20 rpm steps and then back to 100 rpm at no load. The performance degrades as approaching the very low speed region. Different responses to reference speed change at no-load are shown in Fig. 6. Performance at higher speeds is fairly better than low speed.

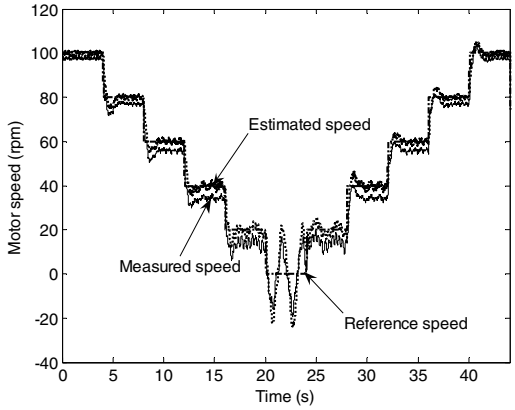

Fig. 5 Sensorless performance for stair case test

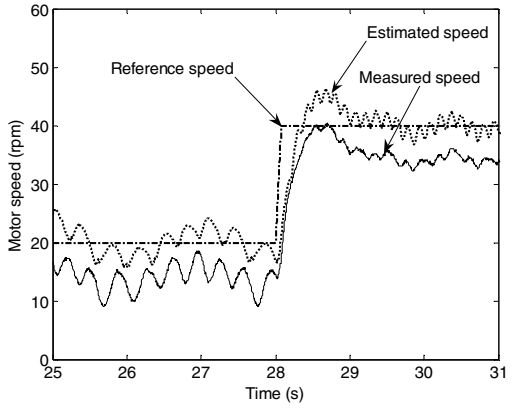

(a)

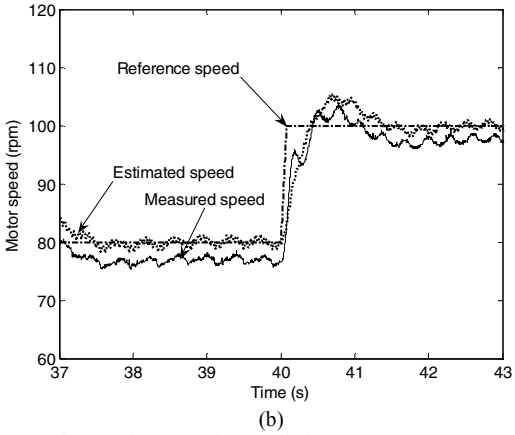

(b)

Fig. 6 Sensorless performance for speed change (a) 20 rpm to 40 rpm (b) 80 rpm to 100 rpm

Fig. 7 shows the sensorless performance for a speed change from 100 rpm to zero speed at no-load. Unstable operation and oscillating speed performance is obtained around the zero speed [19].

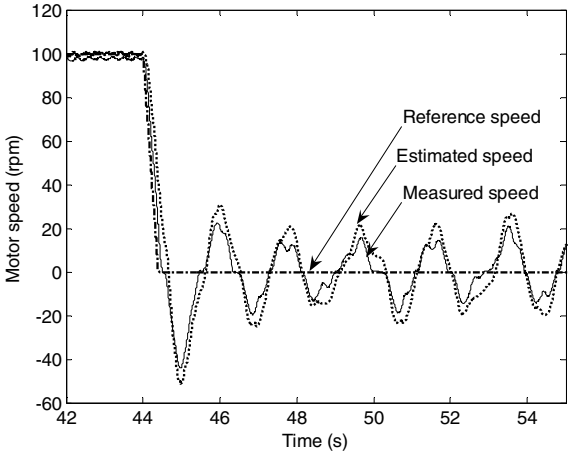

Fig. 7 Sensorless performance at zero speed and no-load

To test the performance of the sensorless drive at very low and zero speed with load. The drive is subjected to speed step down from 20 rpm to 0 rpm in three steps each of 10 rpm at 20% load. Speed control performance is shown in Fig. 8. At a reference speed of 20 rpm, a large steady state error is obtained. At such speeds and below, the MRAS sensorless scheme fails to provide stable operation giving large oscillations. Operation in the regeneration mode is demonstrated in Fig. 9 where the drive is running at -20 rpm at 25% load with large oscillations and instability.

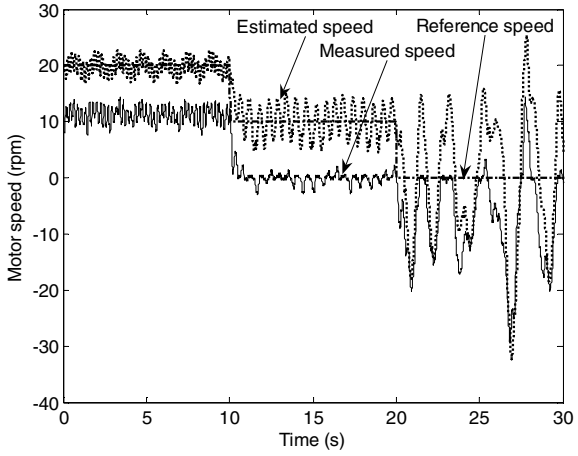

Fig. 8 Sensorless performance at and around zero speed and 20% load

To test the load torque disturbance capability of the sensorless drive at very low speed different levels of load torque are applied at 20 rpm. The drive can hardly reject a disturbance of 25% load with a large steady state error and completely fails to reject a 50% load as shown in Fig. 10.

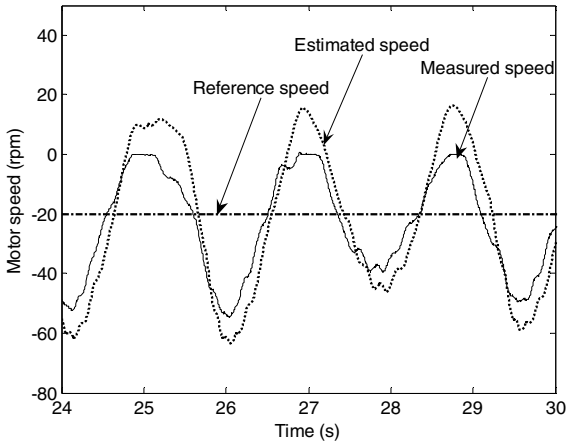

Fig. 9 Sensorless performance at regenerating mode, -20 rpm and 25% load

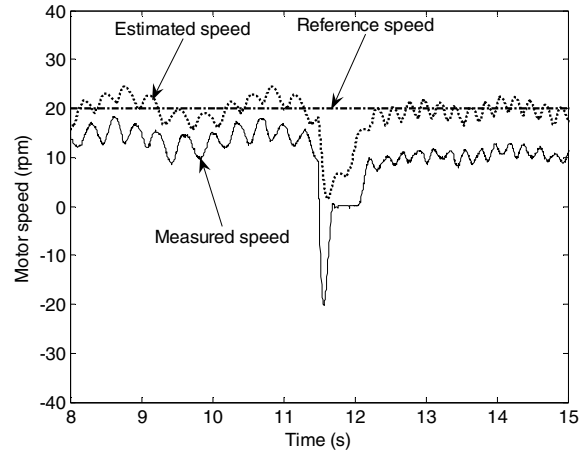

(a)

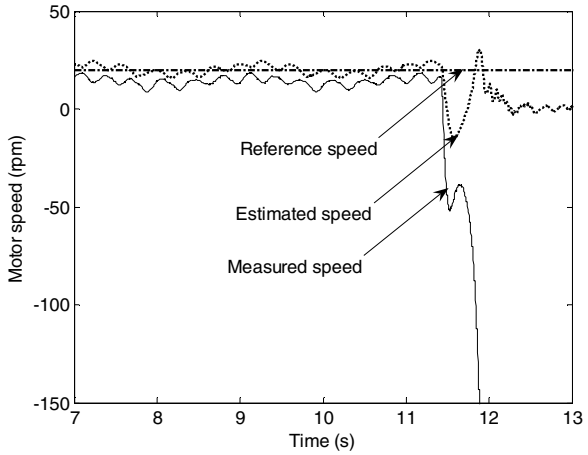

(b)

Fig. 10 Sensorless performance for load torque application at 20 rpm (a) 25% rated load (b) 50% rated load

TABLE I. INDUCTION MOTOR PARAMETERS

Machine parameter	Value	Machine parameter	Value
Rated Power	7.5 [kW]	R_r	0.703 [Ω]
Rated Voltage	415 [V]	L_s	107.73 [mH]
Rated frequency	50 [Hz]	L_m	103.22 [mH]
R_s	0.7767 [Ω]	L_r	107.73 [mH]
Pole number	4	J	0.22 [Kg/m^2]

VI. CONCLUSION

This paper has presented a detailed experimental performance evaluation of a rotor flux MRAS-based sensorless induction motor drive. Both open loop and closed loop sensorless operations have been considered. At open loop, a steady state error in the estimated speed occurs due to parameter mismatch between the machine and the observer as well as inaccurate stator voltage signal. Sensorless performance deteriorates at very low speed for both no-load and loaded conditions with speed oscillations and instability. Worse performance is obtained with high loads where the sensorless drive can even fail to provide a satisfactory and stable response.

ACKNOWLEDGMENT

The authors would like to gratefully acknowledge The Ministry of Higher Education, Arab Republic of Egypt for the financial support of this research project.

REFERENCES

[1] J. W. Finch and D. Giaouris, "Controlled AC Electrical Drives," *IEEE Transactions on Industrial Electronics*, vol. 55, pp. 1-11, 2008.

[2] M. Rashed and A. F. Stronach, "A stable back-EMF MRAS-based sensorless low speed induction motor drive insensitive to stator resistance variation," *IEE Proceedings Electric Power Applications*, vol. 151, pp. 685-693, 2004.

[3] F. Peng and T. Fukao, "Robust speed identification for speed-sensorless vector control of induction motors," *IEEE Transactions on Industry Applications*, vol. 30, pp. 1234-1240, 1994.

[4] C. Schauder, "Adaptive speed identification for vector control of induction motors without rotational transducers," *IEEE Transactions on Industry Applications*, vol. 28, pp. 1054-1061, 1992.

[5] P. Vas, *Sensorless Vector and Direct torque control*. New York: Oxford University Press, 1998.

[6] V. Vasic and S. Vukosavic, "Robust MRAS-Based algorithm for stator resistance and rotor speed identification," *IEEE Power Engineering Review*, vol. 21, pp. 39-41, 2001.

[7] J. Campbell and M. Sumner, "Practical sensorless induction motor drive employing an artificial neural network for online parameter adaptation," *IEE Proceedings Electric Power Applications*, vol. 149, pp. 255 - 260, 2002.

[8] L. Ben-Brahim, S. Tadakuma, and A. Akdag, "Speed control of induction motor without rotational transducers," *IEEE Transactions on Industry Applications*, vol. 35, pp. 844-850, 1999.

[9] B. Karanayil, M. F. Rahman, and C. Grantham, "An implementation of a programmable cascaded low-pass filter for a rotor flux synthesizer for an induction motor drive," *IEEE Transactions on Power Electronics*, vol. 19, pp. 257-263, 2004.

[10] M. Hinkkanen and J. Luomi, "Modified integrator for voltage model flux estimation of induction motors," *IEEE Transactions on Industrial Electronics*, vol. 50, pp. 818-820, 2003.

[11] M. Cirrincione, M. Pucci, G. Cirrincione, and G. Capolino, "A new adaptive integration methodology for estimating flux in induction machine drives," *IEEE Transactions on Power Electronics*, vol. 19, pp. 25-34, 2004.

[12] Q. Gao, C. S. Staines, G. M. Asher, and M. Sumner, "Sensorless speed operation of cage induction motor using zero drift feedback integration with MRAS observer," in *Proc. European Conference on Power Electronics and Applications (EPE 2005)*, 2005.

[13] C. Lascu, I. Boldea, and F. Blaabjerg, "A modified direct torque control for induction motor sensorless drive," *IEEE Transactions on Industry Applications*, vol. 36, pp. 122-130, 2000.

[14] M. Cirrincione and M. Pucci, "An MRAS-based sensorless high-performance induction motor drive with a predictive adaptive model," *IEEE Transactions on Industrial Electronics*, vol. 52, pp. 532- 551, 2005.

[15] M. Cirrincione, M. Pucci, G. Cirrincione, and G. A. Capolino, "Sensorless Control of Induction Machines by a New Neural Algorithm: The TLS EXIN Neuron," *IEEE Transactions on Industrial Electronics*, vol. 54, pp. 127 - 149, 2007.

[16] M. Comanescu and L. Xu, "Sliding mode MRAS speed estimators for sensorless vector control of induction machine," *IEEE Transactions on Industrial Electronics*, vol. 53, pp. 146-153, 2006.

[17] J. Holtz and J. Quan, "Drift and parameter compensated flux estimator for persistent zero stator frequency operation of sensorless controlled induction motors," *IEEE Transactions on Industry Applications*, vol. 39, pp. 1052-1060, 2003.

[18] I. Kumara, "Speed sensorless field oriented control for induction motor drive," PhD Thesis, Newcastle University, UK, 2006.

[19] J. Holtz and J. Quan, "Sensorless vector control of induction motors at very low speed using a nonlinear inverter model and parameter identification," *IEEE Transactions on Industry Applications*, vol. 38, 2002.

[20] M. Gallegos, R. Alvarez, C. Nunez, and V. Cardenas, "Effects of bad currents and voltages acquisition on speed estimation for sensorless drives," in *Proc. The Electronics, Robotics and Automotive Mechanics Conference (CERMA'06)*, 2006.

[21] S. H. Kim, T. S. Park, J. Y. Yoo, G. T. Park, and N. J. Kim, "Dead time compensation in a vector-controlled induction machine," in *Proc. Power Electronics Specialists Conference (PESC 98)*, 1998.

[22] L. Ben-Brahim, "On the compensation of Dead Time and Zero-Current crossing for a PWM-Inverter-controlled AC servo drive," *IEEE Transactions on Industrial Electronics*, vol. 51, pp. 1113-1117, 2004.

[23] K. Ohyama, G. M. Asher, and M. Sumner, "Comparative experimental assessment for high-performance sensorless induction motor drives," in *Proc. IEEE International Symposium on Industrial Electronics, (ISIE 99)*, 1999.

[24] K. Ohyama, G. M. Asher, and M. Sumner, "Comparative analysis of experimental performance and stability of sensorless induction motor drives," *IEEE Transactions on Industrial Electronics*, vol. 53, pp. 178 - 186, 2006.